New standards of absorbed dose to water under reference conditions by graphite calorimetry for ^{60}Co and high-energy x-rays at LNE-LNHB

Franck Delaunay, Jean Gouriou, J. Daures, Maïwenn Le Roy, Aimé Ostrowsky, Benjamin Rapp, S. Sorel

HAL Id: cea-01831912

https://cea.hal.science/cea-01831912

Submitted on 20 May 2019

PAPER

New standards of absorbed dose to water under reference conditions by graphite calorimetry for ^{60}Co and high-energy x-rays at LNE-LNHB

View the article online for updates and enhancements.

Related content

- Dosimetric standards for photons beams in Canada and France
  Ken Shortt, Carl Ross, Jan Seuntjens et al.

- Direct calibration in megavoltage photon beams using Monte Carlo conversion factor: validation and clinical implications
  Tracy Wright, Jessica E Lye, Ganesan Ramanathan et al.

- Using a dose-area product for absolute measurements in small fields: a feasibility study
  S Dufreneix, A Ostrowsky, M Le Roy et al.

Recent citations

- Large irradiation doses can improve the fast neutron/gamma discriminating capability of plastic scintillators
  Eva Montbarbon *et al*

New standards of absorbed dose to water under reference conditions by graphite calorimetry for ^{60}Co and high-energy x-rays at LNE-LNHB

F Delaunay, J Gouriou, J Daures, M Le Roy, A Ostrowsky, B Rapp and S Sorel

CEA, LIST, Laboratoire National Henri Becquerel (LNE-LNHB), F-91191 Gif-sur-Yvette CEDEX, France

E-mail: franck.delaunay@cea.fr

Abstract

The LNE-LNHB has developed two primary standards to determine the absorbed dose to water under reference conditions (for 10 cm × 10 cm) in ^{60}Co, 6 MV, 12 MV and 20 MV photon beams: a new graphite calorimeter and a water calorimeter. This first paper presents the results obtained with the graphite calorimeter and the new associated methodology. The associated relative standard uncertainty ($k = 1$) of absorbed dose to water is 0.25% for ^{60}Co and lies between 0.32% to 0.35% for MV x-ray beams.

Keywords: absorbed dose to water, graphite calorimetry, high-energy x-rays, PENELOPE, EGSnrc, cobalt-60

(Some figures may appear in colour only in the online journal)

1. Introduction

Calorimetry is used by several National Metrology Institutes (NMIs) and the Bureau International des Poids et Mesures (BIPM) for realizing absorbed dose to water standards. A recent review of the different methods to measure photon absorbed dose can be found in the literature [1]. Some of the NMIs use water calorimetry (METAS—Switzerland, NIST—USA, NRCC—Canada, PTB—Germany, VSL—Netherlands [2–10]) and others use graphite calorimetry (BIPM, ARPANSA—Australia, BEV—Austria, ENEA-INMRI—Italy, NMIJ—Japan, NPL–United Kingdom, VNIIFTRI–Russia [11–24]).

At the LNE-LNHB, the previous absorbed dose to water references were based on the graphite calorimeter GR-8 [25] built in 1984. For a ^{60}Co beam, the absorbed dose to graphite in a homogeneous graphite phantom (30 cm × 30 cm × 20 cm) at a depth of 5 g cm^{-2} was determined from the calorimetric measurements [26, 27]. The absorbed dose to water was derived from the absorbed dose to graphite using transfer dosimeters (ionization chambers and Fricke dosimeters) placed successively in the graphite and water phantoms [28, 29]. The absorbed dose to water for the linac beams was derived from the absorbed dose to water of the ^{60}Co beam using ionization chambers and Fricke dosimeters as transfer instruments placed successively in the ^{60}Co and the linac beams in the water phantoms, with an energy dependence taken from the literature [30]. The corresponding relative uncertainty ($k = 1$) was 0.35% for the ^{60}Co absorbed dose to water rate and was between 0.94% and 1.01% for the calibration coefficient of the reference ionization chamber of the linac beams. In recent years the LNE-LNHB has built new calorimeters: the graphite calorimeter GR-9 (figure 1) [31, 32] in 2006 and a water calorimeter [33]. This paper describes the results obtained with the new graphite calorimeter and the new associated methodology.

2. Absorbed dose to water in a ^{60}Co beam

The reference point for measurements is situated at 1 m from the source and at 5 cm depth (front window included) along the
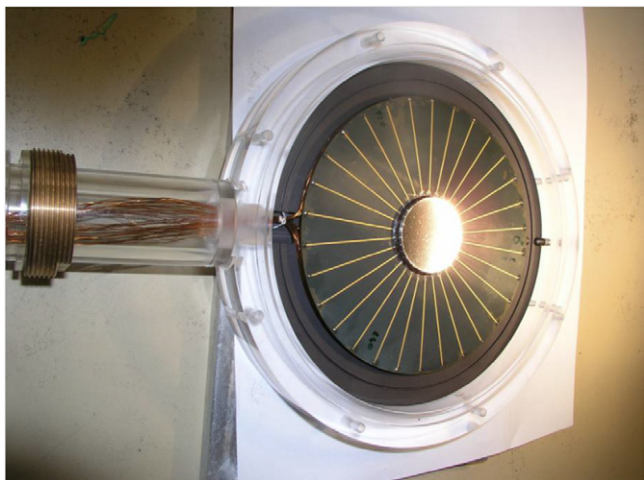
Figure 1. View of the inside of the graphite calorimeter GR-9 (diameter of the core: 1.6 cm). The core and its two jackets are in the gleaming disc in the middle. The golden spokes are connected to the thermistors inside the middle disc and to the reader outside the calorimeter.

beam axis in a water phantom of dimensions 30 cm × 30 cm × 30 cm with a 4 mm front window of polymethyl methacrylate (PMMA). The beam has a diameter of 16 cm (full width at half maximum) at the reference plane.

The methodology to derive the absorbed dose to water from graphite calorimetry measurements has been streamlined in order to reduce the uncertainties and is now based on the mean absorbed dose in the graphite core and Monte Carlo calculations to convert it into absorbed dose to water (no transfer instruments involved).

2.1. Methodology

The method and the results have been presented at the 'Conference on Advanced Metrology for Cancer Therapy' in Braunschweig (29 November 2011) [34]. The ARPANSA has independently developed a very similar method at the same time [23]. The absorbed dose rate to water at the reference point (C) is calculated by using equation (1).

$$\dot{D}_\mathrm{w}(C) = \dot{D}_\mathrm{core} \left[\frac{D_\mathrm{w}(V)}{D_\mathrm{core}} \right]_\mathrm{MC} k_i k_\mathrm{prof}(V) \qquad (1)$$

where $\dot{D}$ means absorbed dose rate and D_w the absorbed dose to water. The mean absorbed dose in the core (D_core) is the quantity measured within the core of the graphite calorimeter GR-9. To simplify the evaluation of uncertainties and avoid unnecessary steps, the mean absorbed dose in the core is used instead of the absorbed dose to graphite at a reference point in a homogeneous graphite phantom at a depth of 5 g cm^{-2}. The ratio of the absorbed dose to water in a volume V surrounding the reference point C, $D_\mathrm{w}(V)$, to the mean absorbed dose in the core is calculated with Monte Carlo codes. The subscript *MC* indicates values calculated by Monte Carlo. The correction factor k_i corresponds to the correction factor for the graphite-core impurities, which are too small to be included in the Monte Carlo simulations (thermistors, conducting wires,

silk threads,...), and $k_\mathrm{prof}(V)$ to the profile correction factor needed to convert $D_\mathrm{w}(V)$ calculated in the finite water volume V at the reference depth (5 cm for the ^{60}Co beam) to $D_\mathrm{w}(C)$ at the reference point.

2.2. Graphite calorimetry

The mean absorbed dose in the core (D_core) is measured within the core of the graphite calorimeter GR-9 inside a graphite phantom of 30 cm × 30 cm × 20 cm (20 cm depth). The depth of the core centre is situated at 4.404 g cm^{-2}.

The calorimeter consists of three concentric bodies (core, jacket, shield), inside the phantom, all made of graphite. These bodies are separated from each other by 1 mm vacuum gaps in order to provide good thermal insulation. The core, the sensitive element, is a flat cylinder of 3 mm thickness and 16 mm diameter. The jacket and the shield thicknesses are 2 mm. These different bodies are suspended by means of three silk threads taut in the median plane of the core. A lateral view of the GR-9 graphite calorimeter is given in figure 2. The radiographs of the three central bodies (front and side views) are given in figure 3.

Six negative temperature coefficient (NTC) thermistors are embedded in the core for the measurements, the thermal control and the electrical calibration. They are in the form of glass-coated beads of 0.35 mm diameter.

The components of the GR-9 core and their respective masses are given in table 1.

The graphite calorimeter can be operated in quasi-adiabatic mode or in constant-temperature mode as previously explained in detail [25]. In the quasi-adiabatic mode, the thermal quantity measured with one thermistor is the temperature rise in the core during the irradiation. The other thermistors are used for the electrical calibration and the thermal control. For the constant-temperature mode, the core is maintained at an assigned temperature by means of controlled and measured electrical power. During irradiation, this measured electrical power is lower because the energy imparted by the ionizing radiation in the graphite is converted into heat. The quantity of interest is the difference of electrical power when the beam is successively off and on. The statistical uncertainties are reduced with this method which is used with the new calorimeters (GR-9 and GR-10).

The earlier GR-8 graphite calorimeter, with a core of the same dimensions, and the most recent one, GR-10, of small cross section adapted for use in the small beams of Intensity-Modulated Radiation Therapy, have been successfully compared with the GR-9 calorimeter used in the present study [32, 35]. The values of absorbed dose to water in ^{60}Co obtained by measurements with the GR-9 and GR-10 calorimeters differed by less than 0.1% with a combined standard uncertainty of 0.3% on their ratio and the GR-8/GR-9 D_core ratios obtained by measurements and by Monte Carlo calculations were within 0.2% of unity, with a statistical uncertainty of 0.3% in the 6 MV and 12 MV beams.

In the present study, the measurements have been made in two campaigns and the mean value of both campaigns is used to determine the mean absorbed dose rate in the core. The type-A uncertainty of $\dot{D}_\mathrm{core}$ is equal to 0.014%.
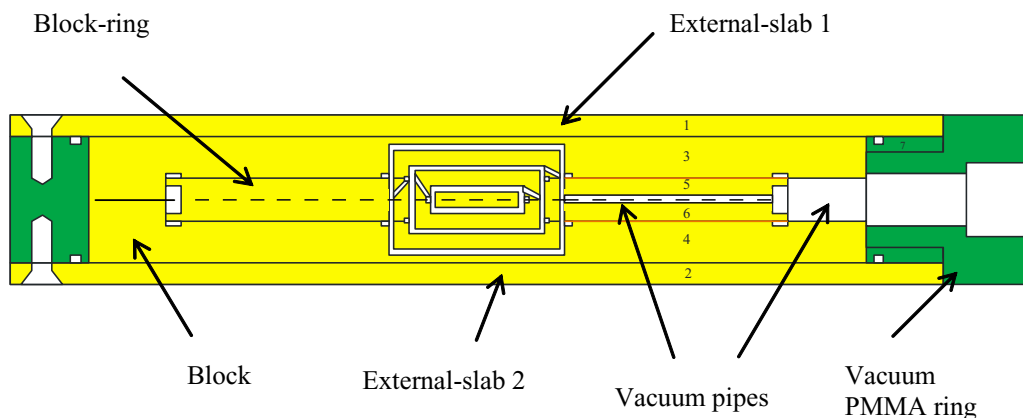
Figure 2. Lateral sectional view of the GR-9 graphite calorimeter.

Block-ring

External-slab 1

Block

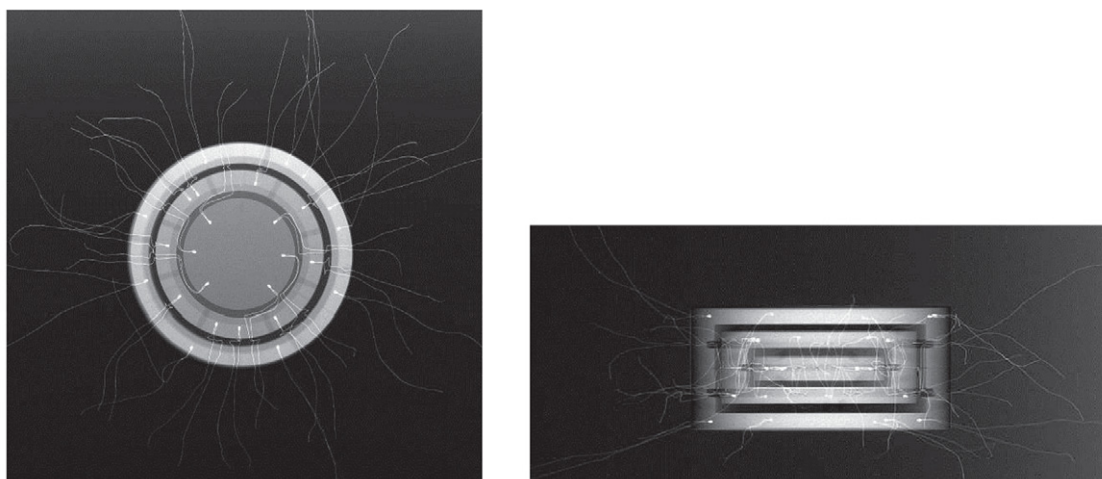External-slab 2

Vacuum pipes

Vacuum PMMA ring

Figure 3. Radiographs of the three internal bodies of the GR-9 graphite calorimeter from the front (at left) and from the side (at right).

Table 1. Masses of the GR-9 core components.

	Mass in the core/g	Uncertainty/g	Mass fraction/10^{-2}
Platinum wires of the thermistors	0.000 90	0.000 09	0.08
Glass	0.000 58	0.000 09	0.05
Sensitive bead	0.000 40	0.000 09	0.04
Mass of glue for the six thermistors	0.003 15	0.000 06	0.30
Mass of glue for the three silk threads	0.000 89	0.000 13	0.08
Total mass of the three silk threads	0.000 39	0.000 04	0.04
Mass of graphite	1.057 43	0.000 02	99.41
Total	1.063 74	0.000 21	100.00

2.3. Monte Carlo calculations

A detailed description of the calculations is presented hereafter, as the calculated dose ratio $[D_w(V)/D_{core}]_{MC}$ is of critical importance in the determination of the absorbed dose to water.

Two different codes were used for the Monte Carlo simulations of the LNE-LNHB ^{60}Co irradiator: EGSnrc v4-r2-3 [36–38] and PENELOPE 2006 [39].

The particles crossing a plane 10 cm ahead of the reference plane (5 cm ahead of the water phantom surface and at 90 cm from the ^{60}Co source) are stored in a phase space file (PSF). The PSFs are created using both BEAMnrc (beam2008rc1) and Penmain_mpi (2.52), a parallelised version

of PENELOPE 2006 [40]. As the cobalt irradiator has a cylindrical geometry, the particles are split 5 times and rotated around the beam axis. The McTwist module [41] was added into BEAMnrc to introduce this type of variance reduction technique. With the PENELOPE code, the simulation of electron transport processes is controlled by specifying values for several parameters: C_1, C_2, W_{CC} and W_{CR}. C_1 and C_2 control, respectively, the average angular deflection produced by multiple elastic scattering of electrons along the step between hard events and the maximum average fractional energy loss in the step. W_{CC} and W_{CR}, respectively, represent the cutoff energy loss for hard inelastic collisions and for hard bremsstrahlung emission. For the PSF creation, the

Table 2. Cutoff energies for the PSF creation.

E_{cut}/keV	Photons	Electrons[a] in air	Electrons[a] not in air
EGSnrc	10	89	89
PENELOPE	10	100	200

[a] Kinetic energy cutoff.

Table 3. Cutoff energies for the dose calculations.

E_{cut}/keV	Photons	Electrons[a]
EGSnrc	10	10
PENELOPE	5	50

[a] Kinetic-energy cutoff.

PENELOPE values used are $C_1 = C_2 = 0.10$. The parameter values W_{CC} and W_{CR} are set equal to the values presented in table 2. The cutoff energies of both codes are summarized in table 2. Each PSF created contains around 4.5×10^8 particles.

The PSFs are used to calculate $D_w(V)$ and D_{core}. The particles in the PSF are split 24 times with EGSnrc (NRCYCL parameter in the DOSRZnrc program) and 25 times with Penmain_mpi. The cutoff energies are summarized in table 3. The mean excitation energies of graphite (calorimeter) and water were taken as equal to 78 eV and 75.0 eV respectively (default values) [42] in both codes. The values of other parameters specific to each Monte Carlo code are taken as identical to those described for the LNE-LNHB high-energy x-ray beams study (see section 3.3).

The volume of water V centred on the reference point C has a cylindrical shape with its revolution axis identical to the beam axis. The cylinder diameter is 16 mm and its thickness is 3 mm (identical to the calorimeter core). The water phantom PMMA walls have a thickness of 15 mm except on the beam axis where the thickness is only 4 mm within a diameter of 12 cm.

The results of the calculations of $[D_w(V)/D_{core}]_{MC}$ are summarized in table 4. The uncertainties (in parentheses) correspond only to type-A uncertainties ($k = 1$) from the calculations. The two code results are in agreement to better than 0.1%. The weighted mean of both code results is chosen for the calculations of the absorbed dose to water. The type-A relative uncertainty for the weighted mean is conservatively taken equal to the largest uncertainty value obtained with the standard deviation of the sample or with the standard deviation of a weighted mean. The type-B relative uncertainty on the dose ratio is evaluated to be 0.2% based on comparisons between calculated and measured dose ratios [43].

Calculations have also been done for a cylindrical volume of water V with a diameter of 2 cm instead of 1.6 cm. The ratio between the two code results is then 1.0007 instead of 1.0006.

2.4. Correction factors

The impurity correction factor k_i takes into account all the details in the core that are not included in the simulation (for example thermistors, silk wires and resin). They are determined by considering that the impurities within the core

are replaced by graphite and the impurities external to the core are replaced by vacuum (thermistor wires and silk threads). The calculation is derived from general cavity theory. The Monte Carlo calculation of the photon and electron spectra allows the estimation of the mean mass energy absorption coefficients and mass stopping powers. The value of the correction factor and its uncertainty are given in table 5.

The profile correction factor in the water volume V (thickness 3 mm, diameter 16 mm), $k_{prof}(V) = D_w(C)/D_w(V)$ is divided into two terms: a longitudinal one (along the beam axis) and a radial one (perpendicular to the beam axis). The beam is assumed to have cylindrical symmetry along the beam axis and around the reference point in the water volume V. Along the beam axis, the longitudinal correction is assumed to be equal to unity with a negligible uncertainty. The radial correction (on a disc with a diameter of 16 mm) is calculated based on the horizontal (X) and vertical (Y) profiles measured inside the water phantom with a small volume ionization chamber. The profile measurements X and Y are symmetrised, and a radial profile (R) calculated from the horizontal and vertical profiles: $R = (X + Y)/2$. The radial profile R is fitted with a polynomial function g (easy to integrate) and $k_{prof}(V)$ is calculated with equation (2).

$$k_{prof}(V) = \frac{R(C)}{\int_0^{r_{max}} g(r)\, r\, dr / \int_0^{r_{max}} r\, dr} \qquad (2)$$

with r_{max} radius of the disc and $R(C)$ value of the radial profile R at the reference point C. The type-A uncertainty is calculated from the measurement reproducibility at point C. The type-B uncertainty is evaluated from the difference between the same calculations with R taken equal to X or to Y as extreme cases, plus 0.02% due to the method. In the ^{60}Co beam with the cylindrical symmetry, X and Y are very similar.

It is possible to compare the products $[D_w(V)/D_{core}]_{MC}k_{prof}(V)$ for the volumes V with the diameters of 1.6 cm and 2 cm. The difference is less than 3 parts in 10^4.

3. Absorbed dose to water in a linac photon beam

The method is very close to the one described in section 2 with a few notable differences. Instead of relying on irradiation time, radiation monitors are used. Instead of calculating a dose rate, a reference ionization chamber is calibrated in the water phantom. This work has been carried out in the 6 MV, 12 MV and 20 MV beams of the Saturne 43 medical linear accelerator at the LNE-LNHB laboratory. The reference point is situated at 10 cm depth (4 mm front window of PMMA within a square of 12 cm side included) along the beam axis in a water phantom of 30 cm × 30 cm × 30 cm.

3.1. Methodology

The calibration coefficient for absorbed dose to water at the reference point (N_{Dw}) is calculated using equation (3):

$$N_{Dw} = \frac{D_{w/mu}(C)}{Q^*_{w/mu}} = \frac{D_{core/mu}}{Q^*_{w/mu}} \left[\frac{D_w(V)}{D_{core}} \right]_{MC} k_i k_{prof}(V)$$

$$(3)$$

Table 4. Calculated ratio $[D_w(V)/D_{core}]_{MC}$ for ^{60}Co.

PENELOPE	EGSnrc	PENELOPE/EGSnrc	Weighted mean	Type A[a]/10^{-2}	Type B[a]/10^{-2}
1.0414 (12)	1.0408 (18)	1.0006 (20)	1.0412	0.094	0.2

[a] Relative standard uncertainties.

Table 5. Correction factors and standard uncertainties.

|		Type A[a]/10^{-2}	Type B[a]/10^{-2}
k_i	0.9992	—	0.10
$k_{prof}(V)$	1.0002	0.01	0.02

[a] Relative standard uncertainties.

where '/mu' in the subscript means that the quantity is 'per monitor unit'. Q_w is the charge measured by the reference ionization chamber in the water phantom corrected for temperature, pressure and humidity. Q_w^* is the charge Q_w corrected for polarity, recombination and radial anisotropy.

As can be seen in equation (3), the calorimeter measurement results should be linked to the charge of the reference ionization chamber in water as directly as possible. To do this, a device was built with the water and graphite phantoms both placed on a mobile tray that can be easily moved to put one phantom in front of the beam and the other out alternately (figure 4). In this way, it was possible to make measurements in the water phantom with the reference ionization chamber in the morning and the evening, before and after the calorimetric measurements.

To check that the monitor information when the water phantom is irradiated, is equivalent to the monitor information when the graphite phantom is irradiated (possible differences in backscattered radiation from the phantoms), measurements were made consecutively with ionization chambers in the water (Q_w) and the graphite (Q_c) phantoms. The ratio between these charges per monitor unit $(Q_{w/mu}/Q_{c/mu})$ has been examined using different monitors. The preferred monitor is placed at the linac head exit, just outside the direct beam. This external additional monitor is more reliable than the internal one supplied with the linac. However, this internal monitor is located well inside the head so it has less dependence on the backscatter of the phantoms. If there is a difference in backscatter on the external monitor due to phantom differences, the charge ratio will be different when normalized to the internal or to the external monitor. The maximum observed discrepancy was of the order of 1 part in 10^4, which is well within the statistical uncertainties (4 to 7 parts in 10^4).

Another point to be checked was whether locating one phantom close to the other contributes to the detection of more scattered radiation in the irradiated phantom. In the equations below, the notation '$\prime$' means that the measurement is made with one phantom close to the other. To ensure that $D_{core/mu}/Q_{w/mu} = D'_{core/mu}/Q'_{w/mu}$ or $D'_{core/mu}/D_{core/mu} = Q'_{w/mu}/Q_{w/mu}$, measurements with ionization chambers were made in the water phantom ($Q_{w/mu}$) and in the graphite phantom ($Q_{c/mu}$) with and without the other phantom by their side. The charge ratios in table 6 should be larger than one if the
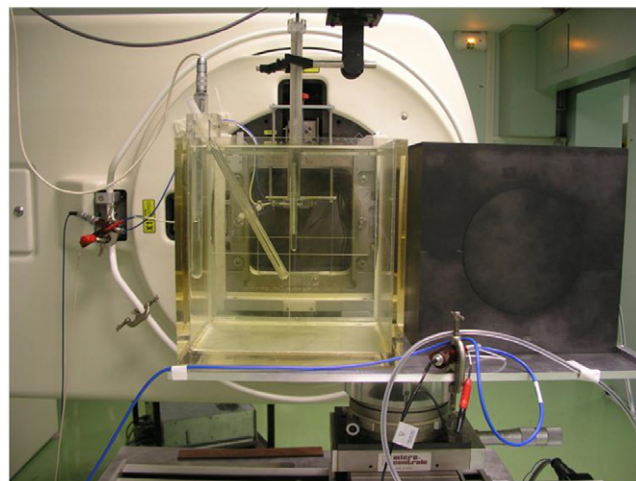
Figure 4. Device allowing the shift of the water and graphite phantom positions in front of the beam. The graphite and water phantoms are positioned on a tray itself on a motorized rail (bottom) that can shift them in front of the beam.

Table 6. $\frac{Q'_{w/mu}}{Q_{w/mu}}$ and $\frac{Q'_{c/mu}}{Q_{c/mu}}$ with their statistical uncertainties.

	$\frac{Q'_{w/mu}}{Q_{w/mu}}$	$\frac{Q'_{c/mu}}{Q_{c/mu}}$
6 MV	1.000 14 (53)	1.000 25 (53)
20 MV	0.999 96 (13)	—

effect is significant. At 6 MV where the scattering should be the largest of the three beams, the measured effect was less than 3×10^{-4}, well within the corresponding statistical uncertainty of 5.3×10^{-4}.

Simulations have been done with EGSnrc to evaluate the effect of the additional phantom on the term $[D_w(V)/D_{core}]_{MC}$. The calculated effect was less than 5 parts in 10^4 for the 6 MV beam and less than 1 part in 10^4 for the 20 MV beam, well within the relative statistical uncertainties of 27×10^{-4} and 12×10^{-4} respectively.

3.2. Graphite calorimetry measurements

The absorbed dose in the core (D_{core}) is measured within the core of the graphite calorimeter GR-9 inside a graphite phantom of 30 cm × 30 cm × 20 cm. The depth of the core centre is situated at 9.379 g cm^{-2}.

One day of measurements of $D_{core/mu}/Q_{w/mu}$ (graphite calorimetric measurements bracketed by the ionization chamber measurements in the morning and evening) is considered as a single measurement for the calculation of uncertainties. The type-B uncertainties in table 7 correspond to the uncertainties on the monitor unit measurement (/mu) and Q_w.

Table 7. Uncertainties of $\frac{D_{\text{core/mu}}}{Q_{\text{w/mu}}}$.

	Type A[a]/10^{-2}	Type B[a]/10^{-2}
6 MV (3 days)	0.031	0.17
12 MV (3 days)	0.028	0.17
20 MV (6 days)	0.051	0.13

[a] Relative standard uncertainties.

3.3. Monte Carlo calculations

A detailed description of the calculations is presented hereafter, as the calculated dose ratio $[D_{\text{w}}(V)/D_{\text{core}}]_{\text{MC}}$ is of critical importance in the determination of the absorbed dose to water.

For each beam and detector studied, the Monte Carlo calculations are divided into two successive steps: creation of PSFs after adjustment of the initial accelerator beam parameters, and dose calculation within the specific geometry of each studied detector (taking into account the volume, shape, density and composition of the various detector components).

3.3.1. Creation of PSFs at the accelerator head output. The purpose of the first step is to determine for a given beam, i.e. with a specific nominal energy and irradiation field size, the characteristics of the initial incident electrons upstream of the accelerator head. Among the various adjustable parameters available, the most important are the electron kinetic energy and the electron impact location on the titanium sheet separating the vacuum of the accelerating cavities from the ambient air in the irradiation room. The incident electron location and kinetic energy distributions are assumed to be Gaussian. In practice, a PSF with a reduced number of particles is generated and used to calculate the beam axis depth-dose distribution and the dose radial anisotropy at 10 cm depth into a 30 cm × 30 cm × 30 cm water-filled tank volume. A maximum of 3 to 4 attempts with different parameter sets (specific electron initial energy and location distributions) are performed for a given beam. The set of parameters which gives the best agreement in terms of radial anisotropy and depth-dose distribution with experimental measurements is considered to correspond to the reference initial parameters for the studied beam. This approach is used concurrently for both Monte Carlo codes used in this study. Therefore, the set of initial parameters can be slightly different from one code to another. Then one PSF of larger dimension is generated according to the initial reference parameter set. The created PSF contains between 150×10^6 and 800×10^6 particles.

Two different codes were used for the Monte Carlo calculations of the SATURNE 43 linear accelerator: EGSnrc v4-r2-2–5 [36, 38] in association with BEAMnrc (beam2007), and PENELOPE 2004 [44]. The calculations have been made on a processor cluster. To run PENELOPE on several processors without overlapping of the random number sequences, seed numbers sufficiently apart in the random sequence were chosen to begin each calculation on a different processor.

The Monte Carlo programs used in this study are shown in table 8:

Table 8. Monte Carlo programs.

Code	PSF creation	Dose calculation
BEAMnrc/EGSnrc	BEAMnrc/DOSXYZnrc	DOSRZnrc
PENELOPE	PSF/Dose3D	Modified/ Pendoses

Table 9. Cutoff energies for the PSF creation.

E_{cut}/keV	photons	Electrons[a] in air	Electrons[a] not in air
EGSnrc	10	189	189
PENELOPE[b]	20/50	500/1000	500/1000

[a] Kinetic energy cutoff.

[b] The lower cutoff energies are for the 6 MV beam.

The DOSXYZnrc and DOSRZnrc programs are associated respectively with the BEAMnrc distribution and EGSnrc code. More complete information is available through their respective user manuals (DOSXYZnrc [45], DOSRZnrc [37]). The PSF and Dose3D programs were developed for previous calculations made at LNE-LNHB [43, 46]. The modified Pendoses program dedicated to the dose calculation corresponds to the Dose3D program except for the scoring areas. The energy depositions are not partitioned in voxels, but in the volumes of the detectors such as the core of the graphite calorimeter (diameter 16 mm, thickness 3 mm) or the water volume *V* around the reference point (diameter 16 mm, thickness 3 mm).

For the PSF creations, the parameters of the EGSnrc code were set to the default values except for three parameters. The pair angular distribution is based on formula 2BS of Koch and Motz [47]. The Bremsstrahlung events were simulated on the basis of the National Institute of Standards and Technology (NIST) differential Bremsstrahlung cross sections [48, 49] and the value of the maximum electron step length, *SMAX*, is set equal to 5 cm.

For the PSF creation, the PENELOPE values used are $C_1 = C_2 = 0.10$ and $W_{\text{CC}} = 10$ keV, $W_{\text{CR}} = 50$ keV. The cutoff energies of both codes are summarized in table 9.

The variance reduction techniques used with PENELOPE are those developed by Mazurier *et al* [50]. They artificially increase the number of created Bremsstrahlung photons and the flux of photons towards the beam aperture. The values of the parameters *FMFP* (forced mean free path) and *PKILL* (killing probability) are identical to those taken by Mazurier (*FMFP* = 0.006 cm for 12 MV and 20 MV, 0.005 cm for 6 MV, *PKILL* = 0.9). The value of the parameter *NSPLIT* (splitting number) is set equal to 5.

The directional Bremsstrahlung splitting (DBS) is called with the BEAMnrc program. Each Bremsstrahlung photon is split into 1500 particles (parameter *IBRSPL*). Moreover, at the flattening filter level, the electrons are split with the same factor and redistributed with radial symmetry about the beam axis. The global cutoff energy value for electron range rejection, *ESAVE*, is set equal to 2 MeV.
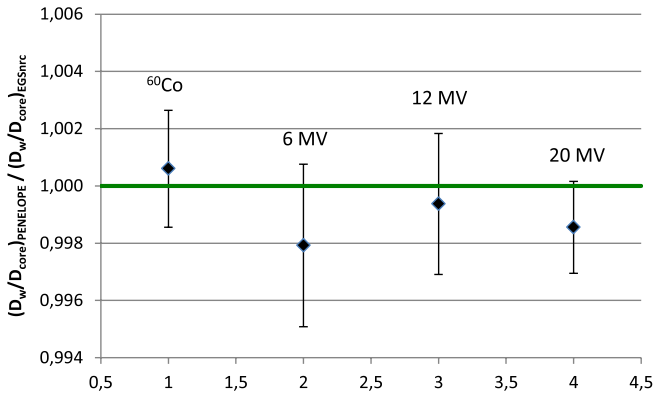
3.3.2. Dose calculations. For the dose calculations, the effects of electron impact ionization (inner shell vacancies) and

Table 10. $[D_w(V)/D_{core}]_{MC}$.

	PENELOPE	EGSnrc	PENELOPE/EGSnrc	weighted mean	Type A[a]/10^{-2}	Type B[a]/10^{-2}
6 MV	1.0123 (25)	1.0144 (14)	0.9979 (28)	1.0139	0.147	0.2
12 MV	1.0477 (21)	1.0484 (14)	0.9994 (25)	1.0482	0.114	0.2
20 MV	1.0631 (15)	1.06467 (85)	0.9986 (16)	1.0643	0.102	0.2

[a] Relative standard uncertainties.

Figure 5. Ratios of PENELOPE and EGSnrc calculations for different beam qualities: $(D_w/D_{core})_{PENELOPE}/(D_w/D_{core})_{EGSnrc}$. Only type-A uncertainties are shown ($k = 1$).

Table 11. Impurity correction factors.

	k_i	u^a / 10^{-2}
6 MV	0.9971	0.1
12 MV	0.9968	0.1
20 MV	0.9967	0.1

[a] Relative standard uncertainties.

Rayleigh scattering are taken into account in the DOSRZnrc program. The EGS value of global energy loss constraint, *ESTEPE*, is set equal to 0.04.

The PENELOPE selected parameter values for the modified Pendoses program are $C_1 = 0.15$, $C_2 = 0.10$ and $W_{CC} = W_{CR} = 5$ keV. The maximum allowed step length between hard interactions of electrons and positrons, *DSMAX*, is set to ensure that, on average, there will be more than 20 soft events along a typical electron/positron track within specific regions (i.e. the sensitive part of the detector).

The cutoff energies of both codes are the same as those used for ^{60}Co and are summarized in table 3.

Given the square shape of the radiation beam, the effective number of particles in the PSF created by the PENELOPE code has been multiplied by a factor of 4 by considering the particle and its three symmetrical counterparts. The number *NSPLIT* of identical particles used with the Russian roulette method is set equal to 10.

The only variance reduction technique used by the DOSRZnrc program is to reuse each particle stored into the PSF files *NRCYCL* times, with *NRCYCL* set equal to 30.

The results of the calculations of $[D_w(V)/D_{core}]_{MC}$ are summarized in table 10. The absolute uncertainties (in parentheses) correspond only to type-A uncertainties ($k = 1$). The results of the two codes agree within uncertainties, the largest observed discrepancy being 0.21% (figure 5). PENELOPE and EGSnrc simulations have also been compared on the occasion of a comparison in absorbed dose to water between the BIPM and the NRCC [51]. The product of $[D_w(V)/D_{core}]/[D_{cav,c}/D_{cav,w}]$ with D_{cav}, the mean dose in the cavity of an ionization chamber positioned in the graphite ($D_{cav,c}$) and in the water ($D_{cav,w}$) phantoms was calculated with both codes for different beams. The differences (between

0.05% and 0.24%) were similar to those observed in this study. The weighted mean of both code results is chosen for the calculation of absorbed dose to water. As for ^{60}Co, the corresponding type-A uncertainty is taken equal to the largest uncertainty evaluation obtained with the standard deviation of the sample or with the standard deviation of a weighted mean. The type-B uncertainty of the dose ratios is evaluated to be 0.2% based on comparisons between calculated and measured dose ratios [43].

Calculations have also been done for a cylindrical volume V of water with a diameter of 2 cm instead of 1.6 cm. Again the two codes agree within uncertainties, the largest observed discrepancy being 0.25%.

3.4. Correction factors

The impurity correction factor k_i takes into account all the details in the core that are not included in the simulation (for example thermistors, silk wires, resin). The determination of this correction factor is described in section 2.4. Its value and the associated uncertainty are given in table 11.

The profile correction factor on the water volume V, $k_{prof}(V) = D_w(C)/D_w(V)$ is treated as in section 2.4. Its value and the associated uncertainties (type A and type B) are given in table 12. The profile correction factors have also been determined in the 6 MV beam with a diamond detector (same methodology but smaller detector) and with EBT3 films (2D measurements) and the results are in agreement within one statistical standard deviation.

It is possible to compare the products $[D_w(V)/D_{core}]_{MC}k_{prof}(V)$ for the volumes V with the diameters of 1.6 cm and 2 cm. The differences are less than 1 part in 10^3.

4. Results and discussion

4.1. Absorbed dose to water with the graphite calorimeter

For the ^{60}Co beam, the different components necessary to calculate the absorbed dose rate to water are summarized in table 13. k_{asym} corrects for the slight asymmetry when the calorimeter is irradiated from the front or from the back. This asymmetry may come from density variations in the graphite

Table 12. Profile correction factors on V.

	$k_{\text{prof}}(V)$	Type A^a/10^{-2}	Type B^a/10^{-2}
6 MV	1.0006	0.076	0.020
12 MV	0.9981	0.076	0.032
20 MV	1.0035	0.076	0.053

^{a} Relative standard uncertainties.

Table 13. $\dot{D}_{\text{w}}(C)$ based on graphite calorimetry for the reference ^{60}Co beam.

$\dot{D}_{\text{core}}$ (Gy/h) 1 July 2004	39.3497 (94)
k_{asym}	1.000 51 (7)
$(D_{\text{w}}(V)/D_{\text{core}})_{\text{MC}}$	1.0412 (23)
$k_{\rho\text{w}}$	1.000 29 (1)
$k_{\text{prof}}(V)$	1.000 22 (22)
$k_{\text{i}}\,\text{GR}-9$	0.9992 (10)
k_{t}	1.388 68 (16)
$\dot{D}_{\text{w}}(C)$ (Gy/h) 1 January 2002	56.91 (14)
$u_{\text{c}}\left(\dot{D}_{\text{w}}(C)\right)/\dot{D}_{\text{w}}(C)$ /10^{-2}	0.25

and has been measured in the ^{60}Co beam. $k_{\rho\text{w}}$ corrects the Monte Carlo calculations which have been done with a water mass density of 1 instead of 0.99823 g cm^{-3} (20 °C). To correct for the decay of the source (k_{t}) between the 1 July 2004 (date close to the measurements in ^{60}Co) and the 1 January 2002 (reference date), a half-life of 5.2711 (8) years is taken [52]. The relative uncertainty of the rate of absorbed dose to water ($k = 1$) is 0.25%. This dose rate of 56.91 (14) Gy/h is higher by 0.19% than the previous reference dose rate based on the graphite calorimeter GR-8 and an experimental graphite-to-water transfer made with Fricke dosimeters and ionization chambers. It should also be noted that the graphite phantom was not of the same density as the one used in this study (1.74 g cm^{-3} previously and 1.85 g cm^{-3} now).

For the linac beams, the different components necessary to calculate the absorbed dose to water calibration coefficient of the reference ionization chamber NE 2571 (# 2791) are summarized in table 14. k_{asym} has been calculated based on the measurements in the ^{60}Co beam. The thickness of the NE 2571 chamber PMMA waterproof sleeve is 0.5 mm. The relative standard uncertainties ($k = 1$) are between 0.32% and 0.35%. The second and third lines present the TPR$_{20,10}$ measurements without and with the recombination correction due to the difference in recombination between 10 cm and 20 cm depth. TPR$_{20,10}$ is the tissue-phantom ratio in water at depths of 20 cm and 10 cm, for a field size of 10 cm × 10 cm and a source-chamber distance of 100 cm. It is used as a beam quality index for high-energy photon radiation. The reference ionization chamber charge is corrected for polarity (k_{pol}), recombination (k_{s}) and radial uniformity (k_{rn}). The determination of k_{rn} is based on the measurement of the vertical profile inside the water phantom with a small volume ionization chamber. These new calibration coefficients are lower by 0.3% at 6 MV, 0.5% at 12 MV and 0.7% at 20 MV than those obtained with the former reference values which had uncertainties of 1% at one standard deviation. The differences between the new and the former references can be considered large particularly at 20 MV. However, the new and former references

are in agreement within one standard deviation. For the references of 1998, the calibration coefficients of the reference ionization chamber were taken as the arithmetic mean of the ionization chamber calibration coefficients determined with calculated ionization chamber k_{Q} and with Fricke dosimeter k_{Q} factors. The ionization chamber k_{Q} factors were taken from the literature [53] with an uncertainty of 1.57% and for the Fricke dosimeter k_{Q} factors [54], a variation of the chemical yield with energy was taken into account [55], with a resulting uncertainty on k_{Q} of 0.55% for 6 MV, 0.83% for 12 MV and 0.95% for 20 MV. The uncertainty on the k_{Q} factors cover the differences with the new calibration coefficient values.

4.2. k_{Q} values for ionization chambers

The linac reference ionization chamber NE 2571 has also been calibrated in the ^{60}Co beam allowing experimental k_{Q} value determinations for the chamber and its sleeve. The thickness of the reference NE 2571 chamber PMMA waterproof sleeve is 0.5 mm. The LNE-LNHB k_{Q} values corresponding to the previous methodology described in the introduction are shown in figure 6 (LNHB 1998) with crosses '+' and without uncertainties for clarity as these standard uncertainties are between 0.87% and 1.1%. The new points are represented with 'x' (uncertainties between 0.41% and 0.44%) and are lower than the previous ones. The protocol TRS-398 [56] proposes uncertainties of 1%. The calculations of Muir and Rogers [57] with uncertainties of 0.28% (if W, mean energy expended in air per ion pair formed, is assumed constant) or 0.57% (if W is not constant) are closer to our k_{Q} as well as the calculations of Wulff *et al* [58] with uncertainties between 0.3% (6 MV) and 0.5% (24 MV) [59]. The thickness of the PMMA waterproof sleeve was taken equal to 1 mm for the calculations. Compared to the experimental points [7, 60–62] all based on water calorimetry, the new k_{Q} values obtained for the reference NE 2571 ionization chamber are in the low region. The different thicknesses of the waterproof sleeves can partly explain the k_{Q} value differences.

4.3. Comparisons

The LNE-LNHB regularly participates in key comparisons of absorbed dose to water for ^{60}Co beams with the BIPM [63]. The previous comparison occurred in April 2013 and the ratio of the absorbed dose to water of LNE-LNHB and BIPM standards was 0.9971 (39). Using only the graphite calorimeter GR-9 and assuming that nothing else changed, the ratio would have been 0.9976 (40).

The BIPM has started a comparison programme with its graphite calorimeter in high-energy photon beams [51, 64–67] of the linacs of primary standard laboratories. The comparison with LNE-LNHB at 6 MV, 12 MV and 20 MV took place in March 2012 [65]. The ratios of the absorbed dose to water of LNE-LNHB and BIPM standards were 0.9952 (44), 0.9948 (47) and 0.9938 (50) for the 6 MV, 12 MV and 20 MV beams respectively. Using only the graphite calorimeter GR-9 and assuming that nothing else changed, the ratios would have been 0.9965 (48), 0.9943 (50) and 0.9952 (52).

Table 14. $N_{Dw}(C)$ of the reference ionization chamber (NE 2571 # 2791) based on graphite calorimetry.

	6 MV	12 MV	20 MV
$TPR_{20,10}$ without k_s	0.676 86 (35)	0.749 19 (38)	0.783 61 (40)
$TPR_{20,10}$ with k_s	0.676 43 (38)	0.748 28 (41)	0.782 47 (42)
$\left[\frac{D_{core/um}}{Q_{w/um}(Rf)}\right]$ (Gy/C)	$4.4110(75) \times 10^7$	$4.2236(70) \times 10^7$	$4.1117(57) \times 10^7$
k_{asym}	1.000 50 (20)	1.000 38 (20)	1.000 32 (20)
$(D_w(V)/D_{core})_{MC}$	1.0139 (25)	1.0482 (24)	1.0643 (24)
$k_{\rho w}$	1.000 60 (2)	1.000 45 (1)	1.000 38 (2)
$k_{prof}(V)$	1.000 65 (79)	0.998 14 (82)	1.003 51 (93)
k_i	0.9971 (10)	0.9968 (10)	0.9967 (10)
k_{pol}	0.999 10 (33)	0.999 09 (33)	0.998 98 (33)
k_s	1.002 82 (56)	1.005 46 (56)	1.005 34 (56)
k_{rn}	1.001 11 (79)	0.998 51 (79)	1.004 75 (79)
N_{Dw} (Gy/C)	$4.454(15) \times 10^7$	$4.395(15) \times 10^7$	$4.340(14) \times 10^7$
$u_c(N_{Dw})/N_{Dw}$ /10^{-2}	0.35	0.33	0.32
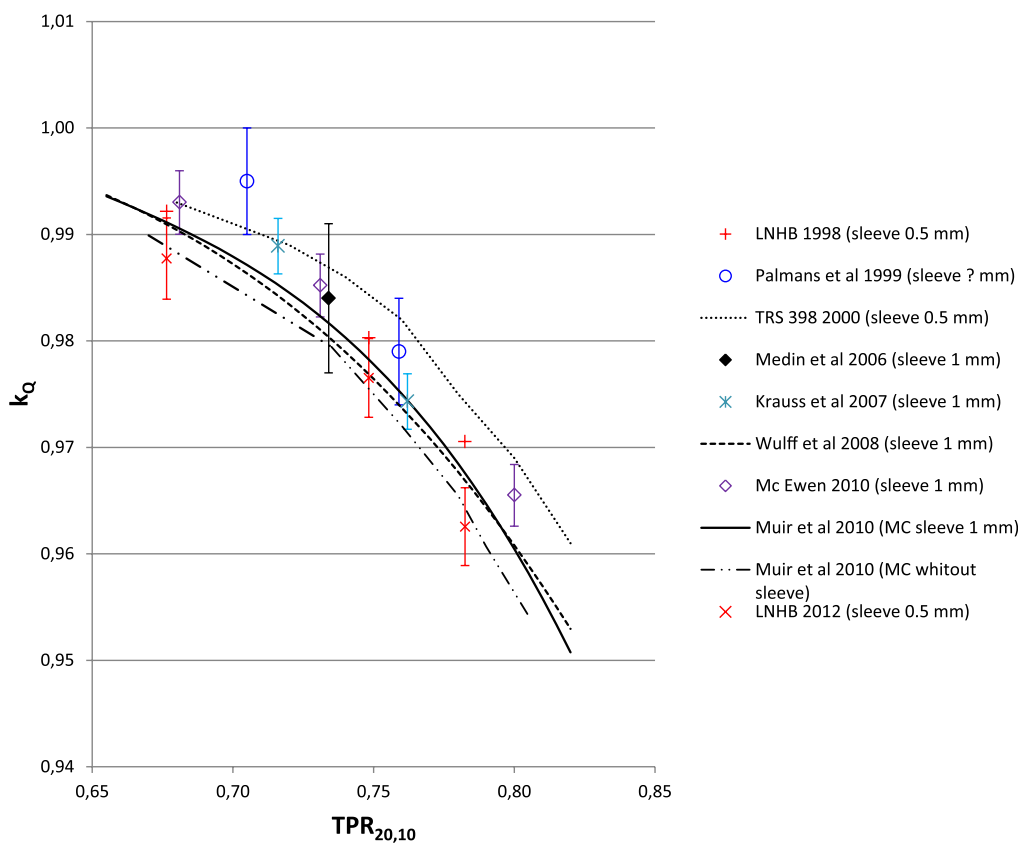
Figure 6. Experimental and calculated k_Q values for a NE 2571 ionization chamber according to different sources.

These results are in very good agreement with those of the ARPANSA [67], which used a very similar method based on graphite calorimetry: 0.9965, 0.9924 and 0.9932 for 6 MV, 10 MV and 18 MV respectively.

Looking at figure 6 at the differences between the k_Q values for high-energy x-rays presented in this study and the experimental values obtained with water calorimetry, and looking at the good agreement between LNHB and ARPANSA via the BIPM.RI(I)-K6 comparisons, one could infer the possible existence of two different sets of results available today according to the type of calorimeter used, i.e. graphite or water. The next comparisons between the BIPM and other primary standards laboratories should confirm or refute this theory.

5. Conclusions

The LNE-LNHB has developed a new graphite calorimeter to determine the absorbed dose to water under reference conditions (10 cm × 10 cm) in ^{60}Co, 6 MV, 12 MV and 20 MV high-energy photon beams. The methodology used to calculate the absorbed dose to water with the graphite calorimeter is now based on the absorbed dose in the core and Monte Carlo calculations. The relative standard uncertainty ($k = 1$) is 0.25% for ^{60}Co and lies between 0.32% and 0.35% for MV x-ray beams. Another paper describing our work based on the water calorimeter will be presented in the future. The results obtained with the two methods will then be compared.

Acknowledgments

The authors would like to thank Bruno Chauvenet and Dr Penelope Allisy-Roberts for their valuable comments and suggestions on this manuscript.

References

[1] Seuntjens J and Duane S 2009 Photon absorbed dose standards *Metrologia* **46** S39

[2] Domen S R 1994 A sealed water calorimeter for measuring absorbed dose *J. Res. Natl Inst. Stand. Technol.* **99** 121

[3] Seuntjens J P, Ross C K, Klassen N V and Shortt K R 1999 A status report on the NRC sealed water calorimeter *NRC Report* PIRS-0584

[4] Medin J, Ross C K, Stucki G, Klassen N V and Seuntjens J P 2004 Commissioning of an NRC-type sealed water calorimeter at METAS using ^{60}Co γ-rays *Phys. Med. Biol.* **49** 4073

[5] Kessler C, Allisy-Roberts P J, Burns D T, Roger P, Krauss A and Kapsch R P 2006 Comparison of the standards for absorbed dose to water of the PTB and the BIPM for ^{60}Co gamma rays *Metrologia* **43** 06005

[6] Krauss A 2006 The PTB water calorimeter for the absolute determination of absorbed dose to water in ^{60}Co radiation *Metrologia* **43** 259

[7] Krauss A and Kapsch R P 2007 Calorimetric determination of k_Q factors for NE 2561 and NE 2571 ionization chambers in 5 cm × 5 cm and 10 cm × 10 cm radiotherapy beams of 8 MV and 16 MV photons *Phys. Med. Biol.* **52** 6243

[8] Krauss A and Kapsch R P 2008 Calorimetric determination of k_Q factors for NE 2561 and NE 2571 ionization chambers in 5 cm × 5 cm and 10 cm × 10 cm radiotherapy beams of 8 MV and 16 MV photons *Phys. Med. Biol.* **53** 1151

[9] Kessler C, Allisy-Roberts P J, Burns D T, Roger P, Prez L A, de Pooter J A and Damen P M G 2009 Comparison of the standards for absorbed dose to water of the VSL and the BIPM for ^{60}Co gamma rays *Metrologia* **46** 06009

[10] Kessler C, Burns D T, Allisy-Roberts P J, McCaffrey J P, McEwen M R and Ross C K 2010 Comparison of the standards for absorbed dose to water of the NRC and the BIPM for ^{60}Co gamma rays *Metrologia* **47** 06016

[11] Witzani J, Duftschmid K E, Stachotinsky Ch and Leitner A 1984 A graphite absorbed dose calorimeter in the quasi-isothermal mode of operation *Metrologia* **20** 73–9

[12] Berlyand V A, Bregadze Y I and Tsuriev S M S 1986 Working standard for unit of absorbed dose of photon ionizing radiation in water *Izmer. Tekh.* **4** 51

[13] DuSautoy A R 1996 The UK primary standard calorimeter for photon-beam absorbed dose measurement *Phys. Med. Biol.* **41** 137

[14] Guerra A S, Laitano R F and Pimpinella M 1996 Characteristics of the absorbed dose to water standards at ENEA *Phys. Med. Biol.* **41** 657

[15] Lye J E, Butler D J, Franich R D, Harty P D, Oliver C P, Ramanathan G, Webb D V and Wright T 2013 Direct MC conversion of absorbed dose to graphite to absorbed dose to water for ^{60}Co radiation *Radiat. Prot. Dosim.* **155** 100

[16] Kessler C, Allisy-Roberts P J, Burns D T, Guerra A S, Laitano R F and Pimpinella M 2010 Comparison of the standards for absorbed dose to water of the ENEA-INMRI (Italy) and the BIPM for ^{60}Co gamma rays *Metrologia* **47** 06002

[17] Kessler C, Allisy-Roberts P J, Steurer A, Baumgartner A, Tiefenboeck W and Gabris F 2010 Comparison of the standards for absorbed dose to water of the BEV Austria and the BIPM for ^{60}Co gamma rays *Metrologia* **47** 06017

[18] Allisy-Roberts P J, Kessler C, Burns D T, Berlyand V and Berlyand A 2010 Comparison of the standards for absorbed dose to water of the VNIIFTRI and the BIPM for ^{60}Co γ-rays *Metrologia* **47** 06003

[19] Kessler C, Allisy-Roberts P J, Burns D T, Roger P, Morishita Y, Kato M, Takata N, Kurosawa T, Tanaka T and Saito N 2011 Comparison of the standards for absorbed dose to water of the NMIJ and the BIPM for ^{60}Co γ-ray beams *Metrologia* **48** 06008

[20] Morishita Y, Kato M, Takata N, Kurosawa T, Tanaka T and Saito N 2013 A standard for absorbed dose rate to water in a ^{60}Co field using a graphite calorimeter at the National Metrology Institute of Japan *Radiat. Prot. Dosim.* **154** 331

[21] Pearce J A D, Shipley D R and Duane S 2011 Transfer of the UK absorbed dose primary standard for photon beams from the research linac to the clinical linac at NPL *Metrologia* **48** 365

[22] Kessler C, Allisy P J, Burns D T, Duane S and Manning J 2012 Comparison of the standards for absorbed dose to water of the NPL (UK) and the BIPM for ^{60}Co γ rays *Metrologia* **49** 06008

[23] Kessler C, Burns D T, Allisy-Roberts P J, Butler D, Lye J and Webb D 2012 Comparison of the standards for absorbed dose to water of the ARPANSA and the BIPM for ^{60}Co γ rays *Metrologia* **49** 06009

[24] Picard S, Burns D T and Roger P 2009 Construction of an absorbed dose graphite calorimeter Rapport BIPM-2009/01 (Sèvres: Bureau International des Poids et Mesures) (www.bipm.org/utils/common/pdf/rapportBIPM/2009/01.pdf)

[25] Daures J and Ostrowsky A 2005 New constant-temperature operating mode for graphite calorimeter at LNE-LNHB *Phys. Med. Biol.* **50** 4035

[26] Daures J, Chauvenet B and Ostrowsky A 1994 State-of-the-art of calorimetry at LPRI *Proc. NPL Calorimetry Workshop 1994 (National Physical laboratory, Teddington, UK)*

[27] Daures J, Ostrowsky A, Gross P, Jeannot J P and Gouriou J 2000 Calorimetry for absorbed dose measurements at BNM-LNHB *Proc. NPL Workshop on Recent Advances in Calorimetric Absorbed dose Standards*, *NPL Report* CIRM-42 p 15 (www.nucleide.org/Publications/Calorimetry_Daures_2000.pdf)

[28] Chauvenet B, Baltès D and Delaunay F 1997 Comparison of graphite-to-water absorbed dose transfers for ^{60}Co photon beams using ionometry and Fricke dosimetry *Phys. Med. Biol.* **42** 2053

[29] Allisy-Roberts P J, Burns D T, Kessler C, Delaunay F and Leroy E 2005 Comparison of the standards for absorbed dose to water of the BNM-LNHB and the BIPM for ^{60}Co γ-rays *Metrologia* **42** 06006

[30] Shortt K, Ross C, Seuntjens J, Delaunay F, Ostrowsky A, Gross P and Leroy E 2001 Comparison of dosimetric standards of Canada and France for photons at ^{60}Co and higher energies *Phys. Med. Biol.* **46** 2119

[31] Ostrowsky A and Daures J 2008 The construction of the graphite calorimeter GR-9 *LNE-LNHB Report* CEA-R-6184 (www.etde.org/etdeweb/servlets/purl/21146686-h2SNPV/21146686.pdf)

[32] Daures J, Ostrowsky A and Rapp B 2012 Small section graphite calorimeter (GR-10) at LNE-LNHB for measurements in small beams for IMRT *Metrologia* **49** S174

[33] Rapp B, Ostrowsky A and Daures J 2011 The LNE-LNHB water calorimeter: measurements in a ^{60}Co beam *Standards, Applications and Quality Assurance in Medical Radiation Dosimetry (IDOS) 2010 (Vienna)* vol 1 (Vienna: IAEA) p 67

[34] Delaunay F, Gouriou J, Le Roy M, Ostrowsky A, Sommier L, Vermesse D, Kapsch R P, Krauss A and Illemann J 2012 Comparison of absorbed dose to water units for Co-60 and

high-energy x-rays between PTB and LNE-LNHB *Metrologia* **49** S203

[35] Daures J and Ostrowsky A 2007 Test of the new GR-9 graphite calorimeter. Comparison with GR-8 *Workshop on Absorbed dose and Air Kerma Primary Standards 2007 (Paris)*

[36] Kawrakow I and Rogers D W O The EGSnrc code system: Monte Carlo simulation of electron and photon transport *NRCC Report* PIRS-701 (EGSnrc v4-r2-2–5: September 2006, EGSnrc v4-r2-3-0: July 2009)

[37] Rogers D W O, Kawrakow I, Seuntjens J P, Walters B R B and Mainegra-Hing E 2005 NRC User codes for EGSnrc *NRCC Report* PIRS-702 (rev B)

[38] Rogers D W O, Walters B and Kawrakow I BEAMnrc Users' Manual *NRCC Report* PIRS-509revK (EGSnrc v4-r2-2–5: September 2006, EGSnrc v4-r2-3-0: July 2009)

[39] Salvat F, Fernandez-Varea J M and Sempau J 2006 PENELOPE-2006: a code system for Monte Carlo Simulation of electron and photon transport *Workshop Proc. 2006 (Barcelona, Spain, 4–7 July 2006)*

[40] Tola F, Poumarède B, Habib B and Gmar M 2009 Optimization of Monte Carlo codes PENELOPE 2006 and PENFAST by parallelization and reduction variance implementation *2nd European Workshop on Monte Carlo Treatment Planning (Cardiff, UK, 19–21 October 2009)*

[41] Bush K, Zavgorodni S F and Beckham WA 2007 Azimuthal particle redistribution for the reduction of latent phase-space variance in Monte Carlo simulations *Phys. Med. Biol.* **52** 4345

[42] Stopping Powers for Electrons and Positrons *ICRU Report* 37 1984 (Washington, DC: International Commission on Radiation Units and Measurements)

[43] Mazurier J 1999 Adaptation du code de Monte Carlo PENELOPE pour la métrologie de la dose absorbée: caractérisation des faisceaux de photons X de haute énergie et calcul de facteurs de correction de dosimètres de référence *Report* CEA-R-5879, Thesis of University Paul Sabatier—Toulouse III, May 1999.

[44] Salvat F, Fernandez-Varea J and Sempau J 2003 PENELOPE—a code system for Monte Carlo simulation of electron and photon transport *Workshop Proc. (Issy-les-Moulineaux, France, 7–10 July 2003)*

[45] Walters B, Kawrakow I and Rogers D W O 2006 DOSXYZnrc Users Manual *NRCC Report* PIRS-794(revB), September 2006

[46] Blazy-Aubignac L 2007 Contrôle qualité des systèmes de planification dosimétrique des traitements en radiothérapie externe au moyen du code Monte Carlo PENELOPE, Thesis of University Paul Sabatier—Toulouse III, September 2007

[47] Motz J W, Olsen H A and Koch H W 1969 Pair production by photons *Rev. Mod. Phys.* **41** 581

[48] Seltzer S M and Berger M J 1985 Bremsstrahlung spectra from electron interactions with screened atomic nuclei and orbital electrons *Nucl. Instrum. Methods Phys. Res.* B **12** 95

[49] Seltzer S M and Berger M J 1986 Bremsstrahlung energy spectra from electrons with kinetic energy from 1 keV to 10 GeV incident on screened nuclei and orbital electrons of neutral atoms with $Z = 1$–100 *At. Data Nucl. Data Tables* **35** 345

[50] Mazurier J, Salvat F, Chauvenet B and Barthe J 1999 Simulation of photon beams from a Saturne 43 accelerator using the code PENELOPE *Phys. Med.* **XV** N3

[51] Picard S, Burns D T, Roger P, Allisy-Roberts P J, McEwen M R, Cojocaru C D and Ross C K 2010 Comparison of the standards for absorbed dose to water of the NRC and the BIPM for accelerator photon beams *Metrologia* **47** 06025

[52] Recommended data by the Decay Data Evaluation Project www.nucleide.org/NucData.htm

[53] Andreo P 1992 Absorbed dose beam quality factors for the dosimetry of high-energy photon beams *Phys. Med. Biol.* **37** 2189

[54] Ma C M and Nahum A E 1993 Dose conversion and wall correction factors for Fricke dosimetry in high-energy photon beams: analytical model and Monte Carlo calculations *Phys. Med. Biol.* **38** 93

[55] Ross C K, Klassen N V and Shortt K R 1994 The development of a standard based on water calorimetry for the absorbed dose to water *Proc. NPL Calorimetry Workshop 1994 (National Physical laboratory, Teddington)*

[56] Technical Report Series no. 398 Absorbed dose Determination in External Beam Radiotherapy International Atomic Energy Agency Vienna 2000

[57] Muir B R and Rogers D W O 2010 Monte Carlo calculations of k_Q, the beam quality conversion factor *Med. Phys.* **37** 5939

[58] Wulff J, Heverhagen J T and Zink K 2008 Monte-Carlo-based perturbation and beam quality correction factors for thimble ionization chambers in high-energy photon beams *Phys. Med. Biol.* **53** 2823

[59] Wulff J, Heverhagen J T, Zink K and Kawrakow I 2010 Investigation of systematic uncertainties in Monte Carlo-calculated beam quality correction factors *Phys. Med. Biol.* **55** 4481

[60] Palmans H, Mondelaers W and Thierens H 1999 Absorbed dose beam quality correction factors k_Q for the NE 2571 chamber in a 5 MV and a 10 MV photon beams *Phys. Med. Biol.* **44** 647

[61] Medin J, Ross C K, Klassen N V, Palmans H, Grusell E and Grindborg J E 2006 Experimental determination of beam quality factors, k_Q, for two types of farmer chamber in a 10 MV photon and a 175 MeV proton beam *Phys. Med. Biol.* **51** 1503

[62] McEwen M R 2010 Measurement of ionization chamber absorbed dose k_Q factors in megavoltage photon beams *Med. Phys.* **37** 2179

[63] Kessler C, Burns D T, Delaunay F and Donois M 2013 Key comparison BIPM.RI(I)-K4 of the absorbed dose to water standards of the LNE-LNHB, France and the BIPM in ⁶⁰Co gamma radiation *Metrologia* **50** 06019

[64] Picard S, Burns D T, Roger P, Allisy-Roberts P J, Kapsch R P and Krauss A 2011 Key comparison BIPM.RI(I)-K6 of the standards for absorbed dose to water of the PTB, Germany and the BIPM for accelerator photon beams *Metrologia* **48** 06020

[65] Picard S, Burns D T, Roger P, Delaunay F, Gouriou J, Le Roy M, Ostrowsky A, Sommier L and Vermesse D 2013 Key comparison BIPM.RI(I)-K6 of the standards for absorbed dose to water of the LNE-LNHB, France and the BIPM in accelerator photon beams *Metrologia* **50** 06015

[66] Picard S, Burns D T, Roger P, Bateman F B, Tosh R E and Chen-Mayer H 2013 Key comparison BIPM.RI(I)-K6 of the standards for absorbed dose to water of the NIST, USA and the BIPM in accelerator photon beams *Metrologia* **50** 06004

[67] Picard S, Burns D T, Roger P, Harty P D, Ramanathan G, Lye J E, Wright T, Butler D J, Cole A, Oliver C and Webb D V 2014 Key comparison BIPM.RI(I)-K6 of the standards for absorbed dose to water of the ARPANSA, Australia and the BIPM in accelerator photon beams *Metrologia* **51** 06006